Check for updates

Comparative study of alterations in phospholipid profiles upon liver cancer in humans and mice†

Haiyan Lu, [ID] [a] Hua Zhang, [ID] [a] Yipo Xiao,[b] Konstantin Chingin,[b] Chao Dai,[c,d] Feng Wei,[e] Nanya Wang,[f] Vladimir Frankevich,[g] Vitaly Chagovets,[g] Fan Zhou*[c] and Huanwen Chen*[b]

Comparative studies of molecular alterations upon cancer between mice and humans are of great importance in order to determine the relevance of research involving mouse cancer models to the development of diagnostic and therapeutic approaches in clinical practice as well as for the mechanistic studies of pathology in humans. Herein, using molecular fingerprinting by internal extractive electrospray ionization mass spectrometry (iEESI-MS), we identified 50 differential signals in mouse liver tissue and 62 differential signals in human liver tissue that undergo significant intensity alterations (variable importance in the project (VIP) >1.0) upon liver cancer, out of which only 27 were common in both mouse and human tissues. Out of the 27 common differential signals, six types of phospholipids were also identified to undergo significant alterations in human serum upon liver cancer, including PC(34:2), PC(36:4), PC(38:6), PC(36:2), PC(38:4) and PC(42:9). Statistical analysis of the relative intensity distribution of these six identified phospholipids in serum allowed confident determination of liver cancer in humans (sensitivity 91.0%, specificity 88.0%, and accuracy 90.0%). Our results indicate that, despite the significant difference in the overall alterations of phospholipid profiles upon liver cancer between humans and mice, the six identified 'core' differential phospholipids of liver cancer found in the liver tissues of both humans and mice as well as in human serum show high potential as a minimal panel for the rapid targeted diagnosis of liver cancer with high accuracy, sensitivity and specificity using direct mass spectrometry (MS) analysis.

1. Introduction

Liver cancer is one of the most common malignant tumors and is the second leading cause of cancer-associated deaths in the world.[1,2] The fight against liver cancer is a long-term and

[a]State Key Laboratory of Inorganic Synthesis and Preparative Chemistry, College of Chemistry, Jilin University, Changchun 130012, P. R. China
[b]Jiangxi Key Laboratory for Mass Spectrometry and Instrumentation, East China University of Technology, Nanchang 330013, P. R. China.
E-mail: chw8868@gmail.com
[c]Department of Hepatobiliary and Pancreatic Surgery, the Second Affiliated Hospital of Nanchang University, Nanchang 330006, P. R. China.
E-mail: nczhoufan@hotmail.com
[d]Department of Hepatobiliary and Pancreatic Surgery, Jiu Jiang No. 1 People's Hospital, Jiujiang 332000, China
[e]Department of Hepatobiliary and Pancreatic Surgery, The First Hospital of Jilin University, Changchun 130021, P. R. China
[f]The Cancer Center, The First Hospital of Jilin University, Changchun 130021, P. R. China
[g]National Medical Research Center for Obstetrics, Gynecology and Perinatology named after Academician V.I. Kulakov of Ministry of Healthcare of Russian Federation, Moscow, 117997, Russian Federation
†Electronic supplementary information (ESI) available. See DOI: 10.1039/d0an01080d

challenging task, which involves the study of pathogenesis, development of preventive, diagnostic and therapeutic tools and exploration of candidate therapeutics.[3–5] Because *in vivo* experimental study on liver cancer typically cannot be performed directly on humans, mouse models of liver cancer are extensively used to reveal molecular mechanisms that could be potentially applied to cancer patients.[4] However, the validity and relevance of mouse models of liver cancer to humans still remain insufficiently explored.[6]

Major efforts have been spent so far at the levels of the genome,[7,8] proteome,[9] and metabolome,[2] whereas phospholipidome was paid much less attention. Biologically, phospholipidome is of particular interest because phospholipids are known to be key mediators for various physiological functions (such as cell signaling, energy fueling and membrane structures). Emerging evidence demonstrates that cancers and diverse human diseases (*e.g.*, Alzheimer's disease, Niemann–Pick disease, Farber disease, Gaucher disease, and Down syndrome) are strongly correlated with the alterations in phospholipid composition.[10–15] Certain phospholipids have been proposed as valuable molecular markers in breast cancer,[16] non-small cell lung cancer,[17] human brain tumors,[18] *etc.* However, the alterations of phospholipids upon liver cancer remain

largely unexplored. Therefore, the study on the relevance of phospholipid alterations between liver cancer mouse models and human patients is of high importance.

In this study, the alterations of phospholipids in different types of tissues (including primary liver cancer tissues, metastases of liver cancer tissue in the lungs, recurrent liver cancer tissues and adjacent tissues) originating from humans and mice suffering from liver cancer were profiled by internal extractive electrospray ionization mass spectrometry (iEESI-MS), which allowed direct characterization of interior chemicals within bulk samples.[13,19–22] For comparison, the phospholipids in the serum samples from liver cancer patients and healthy volunteers were also profiled using direct infusion electrospray ionization mass spectrometry (DI-ESI-MS). The differential signals of liver cancer that are common in serum and liver tissue for both humans and mice were identified using three independent statistical methods: hierarchical cluster analysis (HCA), partial least-squares discriminant analysis (PLS-DA) and orthogonal partial least-squares discriminant analysis (OPLS-DA). In addition, the relevance of molecular alterations between mouse cancer models and human patients was studied using heatmap analysis. Our results reveal substantial differences in the alterations of phospholipids upon cancer between humans and mice but also pinpoint similarly behaving phospholipids. Our results suggest that these similarly behaving phospholipids can be used as a minimal panel for the rapid targeted diagnosis of liver cancer with high accuracy, sensitivity and specificity using direct MS analysis.

2. Experimental section

2.1 Materials and reagents

A total of 302 tissue samples, including 224 mouse tissue samples (including 25 adjacent tissues, 103 primary liver cancer tissues, and 96 metastases of liver cancer tissue in the lungs) from 40 mice and 78 human tissue samples (encompassing 27 adjacent tissues, 11 primary liver cancer tissues, 12 recurrent liver cancer tissues, and 28 metastases of liver cancer tissue in the lungs) from 5 patients, were provided by Second Affiliated Hospital of Nanchang University. 40 blood samples (including 20 blood samples of liver cancer patients and 20 blood samples of healthy volunteers) were provided by The First Hospital of Jilin University. All experiments were performed in accordance with the Guidelines of the Declaration of Helsinki and approved by the ethics committee at Nanchang university and Jilin University. Informed consents were obtained from human participants of this study. All animal procedures were performed in accordance with the Guidelines for Care and Use of Laboratory Animals of Nanchang University and approved by the Animal Ethics Committee of Nanchang University. Collected tissue samples and blood samples were stored at around −80 °C in an ultra-low refrigerator. Methanol (HLPC grade) was bought from ROE

Scientific Inc. (Newark, USA). Deionized water was produced by a Milli-Q water purification system (Billerica, USA).

2.2 Cell cultures

The human hepatocellular carcinoma (HCC) cell line SMMC7721 was purchased from the Shanghai Cell Bank of the Chinese Academy of Sciences (Shanghai, China) and was regularly cultured in Dulbecco's modified essential medium (DMEM) supplemented with 10–12% fetal bovine serum (FBS). The culture was maintained under a 95% air humidified atmosphere containing 5% CO_2 at 37 °C.

2.3 Mouse experiments

Female BALB/c-nu/nu mice (26–30 days old, 15–20 g) were raised at the Medical College of Nanchang University. First, mice were randomly divided into two groups, including primary liver cancer model and lung metastasis of liver cancer model. Then, SMMC7721 cell solution (500 μL, 108 mL^{-1}) was injected into the hepatic subcapsular space of BALB/c-nu/nu mice for the primary liver cancer model, and SMMC7721 cell solution (500 μL, 107 mL^{-1}) was injected into the tail vein of BALB/c-nu/nu mice for the lung metastasis of liver cancer model. Tumors were consistently monitored for 3–4 weeks until they reached 0.4 cm to 0.5 cm in diameter. Finally, 20 case specimens were collected in each group.

2.4 Analysis of tissue by iEESI-MS

The iEESI-MS experiments were carried out using a disposable iEESI source coupled with a linear trap quadruple (LTQ) mass spectrometer (Thermo Scientific, San Jose, CA), with methanol/water (30 : 70) as the extraction solution. The volume of tissue samples was 1 mm^3 (ca. 1.5 mg) for each analysis, and the details of the disposable iEESI source were described in the literature.[23] iEESI-MS data were profiled in the mass range of m/z 50–2000 under positive ion detection mode. The MS instrumental conditions were as follows: the spray voltage of 5.0 kV, the capillary temperature of 200 °C, the tube lens voltage of 100 V, and the capillary voltage of 10 V. The chemical assignments were based on collision-induced dissociation (CID) experiments, high-resolution mass measurement and comparison with earlier literature as well as the search across the Human Metabolome Database (HMDB, http://www.hmdb.ca) and LIPID MAPS (http://www.lipidmaps.org). During CID experiments, precursor ions were isolated with a window width of 1.5 Da, and the normalized collision energy was 10–30%. Other parameters were set as default values of the instrument. For comparison, the phospholipids in the serum samples from liver cancer patients and healthy volunteers were also profiled using DI-ESI-MS, and the details about serum preparation and working conditions of DI-ESI-MS are described in the ESI.†

2.5 Data processing

The Xcalibur raw data arranged using the m/z values as independent variables and the signal intensity as dependent variables were converted to the Microsoft Excel spreadsheet

format. First, all data were scaled and aligned on the basis of a program in Matlab (version 7.8.0, Mathworks, Inc., Natick, MA). Then, the processed data were imported to soft independent modeling of class analogies (SIMCA) (version 13.0, Umetrics, Umeå, Sweden) for PLS-DA, OPLS-DA, and HCA. In HCA, all the mass signal peaks from the mass spectra in the mass range of m/z 700–900 were selected as variables. The group single linkage method was applied to sort samples into clusters. The signal intensities of identified 16 phospholipids with a high variable importance in the project (VIP) value (VIP >1.0) in distinguishing different types of mouse/human tissue samples were extracted for the construction of heatmaps. Random forest (RF) was used for the performance evaluation of potential biomarkers in molecular diagnosis of liver cancer. In RF analysis, the number of decision trees was 500, and the analyzed data were divided into training sets and validation sets at a ratio of 7 : 3. Heatmaps and RF were obtained by using the R programming language (version 3.5.1).

3. Results and discussion

3.1 Direct analysis of human tissue samples by iEESI-MS

The mass spectra of adjacent tissues of primary liver cancer (Fig. 1a), primary liver cancer tissues (Fig. 1b), recurrent liver cancer tissues (Fig. 1c), and metastases of liver cancer tissue in the lungs (Fig. 1d) show the dominant signals of phospholipids in the mass range of m/z 700–900. Based on the high-resolution mass measurement, CID data, search across the HMDB (http://www.hmdb.ca) and LIPID MAPS (http://www.lipidmaps.org) as well as the comparison with earlier literature,[14,24–27] the phospholipids were identified as sphingomyelins (SMs) and phosphatidylcholines (PCs), including m/z 726 [SM(34:1) + Na]$^+$, m/z 742 [SM(34:1) + K]$^+$,

m/z 759 [PC(34:2) + H]$^+$, m/z 773 [PC(32:0) + K]$^+$, m/z 781 [PC(34:2) + Na]$^+$, m/z 783 [PC(36:4) + H]$^+$, m/z 797 [PC(34:2) + K]$^+$, m/z 799 [PC(34:1) + K]$^+$, m/z 825 [PC(36:2) + K]$^+$, m/z 845 [PC(38:6) + K]$^+$, m/z 849 [PC(38:4) + K]$^+$, etc. The identification process and detailed data for the identified phospholipids are shown in Table S1, ESI.†

The iEESI-MS fingerprints of adjacent tissues (Fig. 1a), primary liver cancer tissues (Fig. 1b), recurrent liver cancer tissues (Fig. 1c), and metastases of liver cancer tissue in the lungs (Fig. 1d) showed the presence of the same major PCs and SMs albeit with reproducible variations in the relative abundance. Among dominant PC and SM signals presented in the iEESI-MS spectra of different types of liver cancer tissue samples, m/z 726 [SM(34:1) + Na]$^+$, m/z 742 [SM(34:1) + K]$^+$, m/z 773 [PC(32:0) + K]$^+$, m/z 783 [PC(36:4) + H]$^+$, m/z 799 [PC(34:1) + K]$^+$, m/z 809 [PC(36:2) + Na]$^+$ and m/z 833 [PC(38:4) + Na]$^+$ were previously identified as differential signals between the nontumor region and tumor region of metastatic human-liver adenocarcinoma tissue by desorption electrospray ionization mass spectrometry (DESI-MS).[14] These results demonstrate the high sensitivity of iEESI-MS to distinguish the alterations of phospholipids in different types of liver cancer tissue samples, owing to the unique capability of iEESI to reveal the inner chemicals without tedious sample pretreatment.[19–22]

3.2 HCA of iEESI-MS data collected from human tissue samples

Using HCA, samples were tightly clustered (Fig. 2) on the basis of the similarity of each group of samples without taking into account the information about the class membership.[28,29] Four clusters included primary liver cancer tissues (red clusters), recurrent liver cancer tissues (blue clusters), metastases of liver cancer tissue in the lungs (yellow clusters), and adjacent tissues (green clusters). Besides, the VIP value revealed 62 significant iEESI-MS signals with VIP >1.0 that made the major contribution to the differentiation of the four types of human liver cancer tissue samples (Table S2, ESI†), indicating that iEESI-MS was suitable for the screening of potential biomarkers of liver cancer. The successful HCA clustering
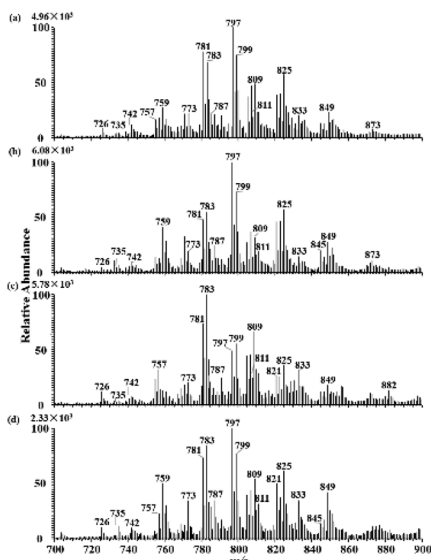

Fig. 1 iEESI-MS spectra of different types of human tissue samples. (a) Adjacent tissues, (b) primary liver cancer tissues, (c) recurrent liver cancer tissues, and (d) metastases of liver cancer tissue in the lungs.
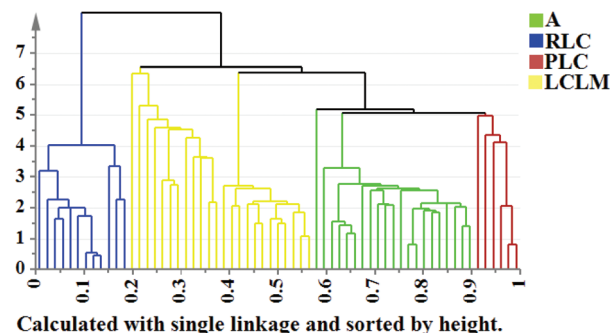

Fig. 2 HCA dendrogram of four types of human liver cancer tissues (note: green clusters represent adjacent tissues (A), blue clusters represent recurrent liver tissues (RLC), red clusters represent primary liver tissues (PLC), and yellow clusters represent metastases of liver cancer tissue in the lungs (LCLM)).

suggests that the information acquired by iEESI-MS could be used to distinguish the differences among the four types of human liver cancer tissues.

3.3 Direct analysis of mouse tissue samples by iEESI-MS

The iEESI-MS mass spectra of adjacent tissues (Fig. 3a), primary liver cancer tissues (Fig. 3b) and metastases of liver cancer tissue in the lungs (Fig. 3c) of mice were collected under the experimental conditions identical to those used for the analysis of human tissue samples. The mass spectra of mouse tissues were dominated by a variety of phospholipids such as m/z 726 [SM(34:1) + Na]$^+$, m/z 742 [SM(34:1) + K]$^+$, m/z 773 [PC(32:0) + K]$^+$, m/z 783 [PC(36:4) + H]$^+$, m/z 787 [PC(36:2) + H]$^+$, m/z 797 [PC(34:2) + K]$^+$, m/z 799 [PC(34:1) + K]$^+$, m/z 809 [PC(36:2) + Na]$^+$, m/z 811 [PC(38:4) + H]$^+$, m/z 821 [PC(36:4) + K]$^+$, m/z 845 [PC(38:6) + K]$^+$, and m/z 873 [PC(40:6) + K]$^+$, showing that iEESI-MS could directly detect phospholipids in mouse tissue samples. Although notable overall variations were found in the signal levels recorded from the three types of mouse tissue samples, the iEESI-MS mass spectra showed reproducible profiles, providing a solid base for reliable differentiation of the samples. More interestingly, the dominant phospholipids signals in iEESI-MS spectra from the tissue of liver cancer in mice (Fig. 3) were nearly identical to the major phospholipid signals obtained from human tissues (Fig. 1).

3.4 PLS-DA of iEESI-MS data collected from mouse tissue samples

PLS-DA is commonly used for the classification and selection of biomarkers.[30] As revealed by the score plot of PLS-DA (Fig. 4a), the molecular patterns obtained by iEESI-MS data from the three types of mouse tissue samples were clearly distinguished into three distinct groups. To further validate the model, 200 random permutation tests (Fig. 4b) were performed, with intercepts R^2 = 0.263 and Q^2 = −0.352, indicating that the model was not over-fitted.[13] Furthermore, the S-plot (Fig. 4c) and VIP value screened 50 signals (VIP >1.0)

Fig. 4 Differential analysis of three types of mouse tissue samples. (a) Score plot of PLS-DA models derived from iEESI-MS data of primary liver cancer tissues (PLC) (green squares), metastases of liver cancer tissue in the lungs (LCLM) (blue squares) and adjacent tissues (A) (red squares), (b) permutation test results (200 permutations) of the PLS-DA model indicated that the model was not over-fitted, and (c) S-plot revealed the potential biomarkers in molecular differentiation of liver cancer.

(Table S2, ESI†), which notably contributed to the molecular differential analysis of the three groups of the tissue samples, including phospholipid signals at m/z 757, m/z 773, m/z 783, m/z 797, m/z 799, m/z 809, m/z 825, m/z 849, *etc.* These data are important for the further search of potential biomarkers of liver cancer. All the three statistical methods (HCA, OPLS-DA, and PLS-DA) employed in this study yielded consistent behavior in identifying the same differential signals. A more clear differentiation for the analysis of human tissue samples was achieved using HCA. A more clear differentiation for the analysis of mouse tissue samples was achieved using PLS-DA.

3.5 Heatmap visualization of 16 phospholipid signals in human and mouse tissue samples

To further compare the alterations of major phospholipids in humans and in the mouse model of liver cancer, the iEESI-MS signal intensities of the 16 phospholipid signals which made the major contribution to the differentiation between different types of cancer tissues according to the VIP value and S-plot in both humans and mice (including m/z 735 [PC(32:0) + H]$^+$, m/z
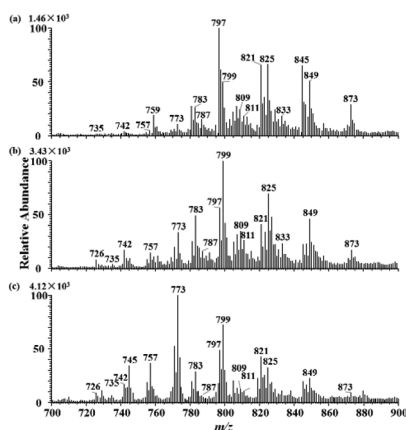
Fig. 3 iEESI-MS spectra of different types of mouse tissues. (a) Adjacent tissues, (b) primary liver cancer tissues, and (c) metastases of liver cancer tissue in the lungs.
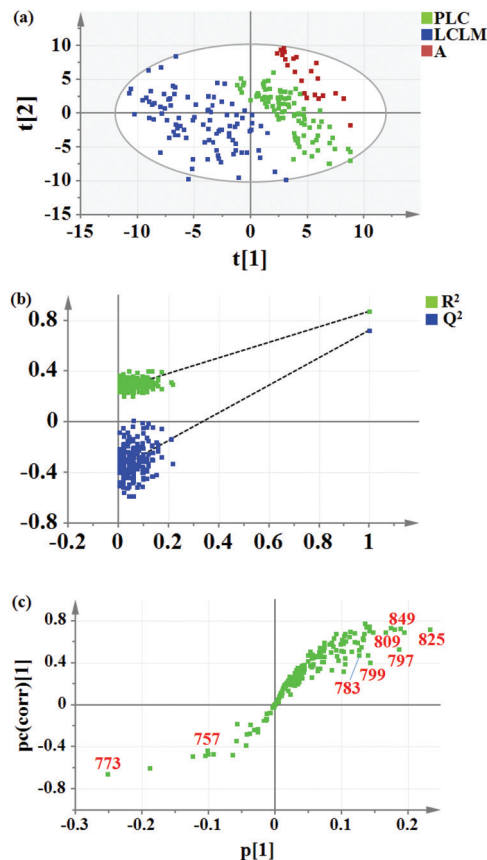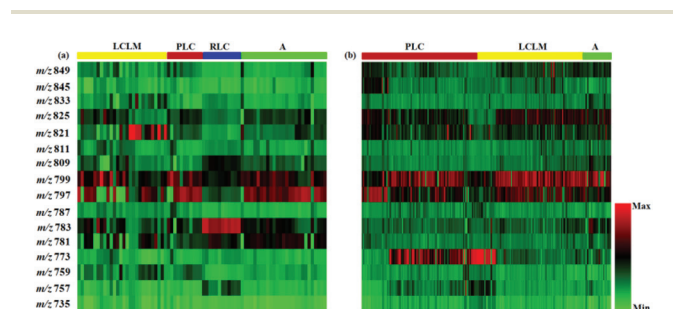
757 [PC(32:0) + Na]$^+$, m/z 759 [PC(34:2) + H]$^+$, m/z 773 [PC(32:0) + K]$^+$, m/z 781 [PC(34:2) + Na]$^+$, m/z 783 [PC(36:4) + H]$^+$, m/z 787 [PC(36:2) + H]$^+$, m/z 797 [PC(34:2) + K]$^+$, m/z 799 [PC(34:1) + K]$^+$, m/z 809 [PC(36:2) + Na]$^+$, m/z 811 [PC(38:4) + H]$^+$, m/z 821 [PC(36:4) + K]$^+$, m/z 825 [PC(36:2) + K]$^+$, m/z 833 [PC(38:4) + Na]$^+$, m/z 845 [PC(38:6) + K]$^+$ and m/z 849 [PC(38:4) + K]$^+$) were extracted for the construction of heatmaps (Fig. 5). The heatmap revealed that the phospholipid signals at m/z 735 [PC(32:0) + H]$^+$, m/z 757 [PC(32:0) + Na]$^+$, m/z 759 [PC(34:2) + H]$^+$, m/z 787 [PC(36:2) + H]$^+$, m/z 809 [PC(36:2) + Na]$^+$, m/z 811 [PC(38:4) + H]$^+$, m/z 833 [PC(38:4) + Na]$^+$, m/z 845 [PC(38:6) + K]$^+$ and m/z 849 [PC(38:4) + K]$^+$ showed consistent relative intensity alterations between adjacent tissues, primary liver cancer tissues and metastases of liver tissues in the lungs in both humans and mice. This further suggests that the major alterations of phospholipids in humans and mice upon liver cancer are largely similar. Also, some phospholipid signals with distinct intensities in each sample, for example, m/z 797 [PC(34:2) + K]$^+$, m/z 799 [PC(34:1) + K]$^+$, and m/z 821 [PC(36:4) + K]$^+$ showed significant alteration in the metastases of liver cancer tissues in the lungs of humans, while m/z 773 [PC(32:0) + K]$^+$, m/z 797 [PC(34:2) + K]$^+$, and m/z 799 [PC(34:1) + K]$^+$ showed prominent changes in the primary liver cancer tissues of mice. For better consistency of our comparative study, the same types of tissue samples should be analyzed for both mice and humans. Unfortunately, owing to the failure of the recurrent liver cancer mouse model in our study, the recurrent liver cancer tissues from mice were not compared with the recurrent liver cancer tissues of humans.

Moreover, changes in phospholipids in Fig. 5 may be of particular interest for deeper understanding the pathogenesis of liver cancer. For instance, PC, as a component of membrane phospholipids, is generated from lysophosphatidylcholine (LPC) under the lysophosphatidylcholine acyltransferase 1 (LPCAT1).[31] Previous study revealed that LPC has abnormal changes during the carcinogenesis of liver cancer, and the
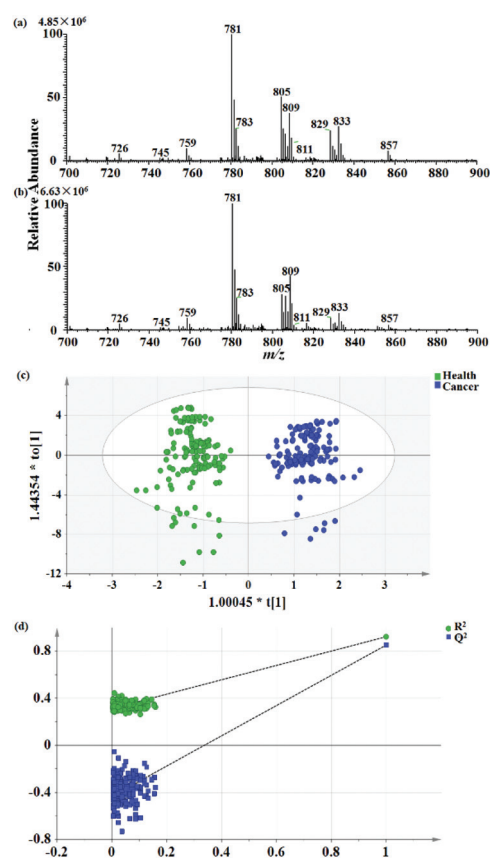
alterations of phospholipid composition are caused by the overexpression of LPCAT1.[27,31] In some cases, the elevated levels of PC species are correlated with malignant transformations in cancer cells, and extracellular membrane vesicles rich in SM could promote angiogenesis in tumor cells. Besides, cell-signaling molecules, such as ceramides, derivatives of the SM species, are involved in cell-signaling cascades that are directly related to tumor survival.[14,32] Therefore, a more comprehensive analysis of the alterations in phospholipids of liver cancer is needed for the better understanding of the molecular mechanism behind cancer progression.

3.6 Analysis of human serum samples by DI-ESI-MS for the cross-proof of the human tissue differentiation by iEESI-MS

To validate the alteration of phospholipids observed in tissue samples by iEESI-MS, the composition of phospholipids in 40 serum samples (including 20 healthy volunteers and 20 liver cancer patients) was analyzed by DI-ESI-MS. The mass spectra of all the serum samples (healthy volunteers (Fig. 6a) and liver

Fig. 6 Differentiation of human serum samples of healthy volunteers and liver cancer patients by DI-ESI-MS analysis. (a) Mass spectrum of serum samples of healthy volunteers, (b) mass spectrum of serum samples of liver cancer patients, (c) OPLS-DA score plot of mass spectral data from serum samples of healthy volunteers (green dots) and liver cancer patients (blue dots), and (d) permutation test results (after 200 permutations) of the OPLS-DA model indicated that the model was not over-fitted.

Fig. 5 Heatmap constructed based on the iEESI-MS signal intensities of identified 16 phospholipids, with a high VIP value in differential analysis of human/mouse tissue samples. (a) Heatmap of human tissue samples and (b) heatmap of mouse tissue samples (note: A represents adjacent tissues, PLC represents primary liver cancer tissues, LCLM represents metastases of liver cancer tissues in the lungs, RLC represents recurrent liver cancer tissues. In the heatmap, rows represent phospholipid species, columns represent samples, and color (from green (the lowest) to red (the highest)) indicates the signal intensity of phospholipids (row) in each sample (column)).

cancer patients (Fig. 6b)) were dominated by the signals of phospholipids, including m/z 726 [SM(34:1) + Na]$^+$, m/z 759 [PC(34:2) + H]$^+$, m/z 781 [PC(34:2) + Na]$^+$, m/z 805 [PC(36:4) + Na]$^+$, m/z 809 [PC(36:2) + Na]$^+$, m/z 857 [PC(42:9) + H]$^+$, *etc.* Note that the mass spectra obtained from healthy volunteers (Fig. 6a) and liver cancer patients (Fig. 6b) all showed identical phospholipid species although with notably different relative abundance for some signals (*e.g.*, m/z 805 and m/z 809). Note that the signal intensity ratios are highly different between serum and liver tissue samples of humans (Fig. 6 *vs.* Fig. 1), which is due to the different phospholipid composition in tissue and in serum. With OPLS-DA, a set of 40 serum samples were completely separated into two groups in the OPLS-DA score plots (Fig. 6c). The OPLS-DA model was further validated by performing 200 random permutation tests (Fig. 6d), which yielded the intercepts R^2 = 0.312 and Q^2 = −0.434, indicating that the OPLS-DA model was properly fitted. Furthermore, 53 signals were selected by setting the threshold VIP >1.0 (Table S2, ESI†). These 53 signals from DI-ESI-MS analysis of human serum made great contribution to separate the healthy volunteers from the liver cancer patients.

A Venn diagram (Fig. 7) was constructed to cross-validate the coverage of differential signals (with a VIP >1.0) between human tissues, mouse tissues and human serum. In detail, a total of 62, 50 and 53 differential signals with a VIP >1.0 were screened from the human tissues, mouse tissues and human serum, respectively. It can be seen from Fig. 7 that 27 differential signals were shared between human tissues and mouse tissues, 20 differential signals were shared between human tissues and human serum, and 14 differential signals were shared between human serum and mouse tissues. Seven signals corresponding to six types of phospholipids (including PC(34:2), PC(36:4), PC(38:6), PC(36:2), PC(38:4) and PC(42:9)) were found in each sample category (mouse tissue, human tissue, and human serum), indicating the high versatility of these signals as differential metabolites for the molecular diagnosis of liver cancer, although the underlying molecular mechanism still remains to be explored in further studies.
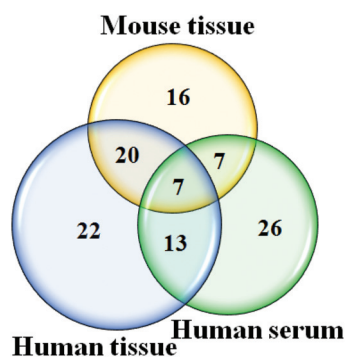

Fig. 7 Venn diagram displays the coverage of differential signals (VIP >1.0) in molecular analysis of mouse tissue samples (yellow circle), human tissue samples (blue circle) and human serum (green circle).

Table 1 The comparison of predictive performance obtained using RF

Chemical information	Sensitivity	Specificity	Accuracy
m/z 700–900	0.96	1.0	0.98
53 signals (VIP >1.0)	0.96	1.0	0.98
7 signals of phospholipids	0.91	0.88	0.9

3.7 Clinical value of the six phospholipids

Although serum alpha-fetoprotein (AFP) has been applied in clinical utility for the detection of liver cancer, only a few biomarkers have so far provided high accuracy and specificity for the early diagnosis of liver cancer.[33,34] Here, the potential value of the 53 signals displayed a VIP >1.0 for the differentiation of healthy volunteers and liver cancer patients in the mass range of m/z 700–900, and seven signals corresponding to the six types of phospholipids (including PC(34:2), PC(36:4), PC(38:6), PC(36:2), PC(38:4) and PC(42:9)) that were found in each sample category (mouse liver tissue, human liver tissue, and human serum) for the molecular diagnosis of liver cancer have been evaluated using RF based on the MS data from serum samples in terms of sensitivity, specificity, and accuracy. RF is a method that relies on model aggregation, which is a family of ensemble data mining tools that avoid overfitting of the trained model.[35] As shown in Table 1, the sensitivity of 96.0%, specificity of 100.0%, and accuracy of 98.0% for liver cancer prediction were obtained using all the molecular information in the full mass range of m/z 700–900. When all the signal features in the mass range of m/z 700–900 are used to predict liver cancer in the RF model, the importance of all the signal features is evaluated (Table S3, ESI†). Surprisingly, similar performance was obtained when using only the seven shared phospholipid signals (sensitivity 91.0%, specificity 88.0%, and accuracy 90.0%). The obtained performance using the seven shared signals of six types of phospholipids is similar to the reported performance of the serum metabolite panel with regard to sensitivity (91% *vs.* 91.6%), but superior with regard to the accuracy (90% *vs.* 87.5%) and specificity (88% *vs.* 72.2%).[36] These results indicate that the six identified 'core' differential phospholipids of liver cancer found in the liver tissues of both humans and mice as well as in human serum show high potential as a minimal panel for the rapid targeted diagnosis of liver cancer with high accuracy, sensitivity and specificity using direct MS analysis. Note that the result presented in Table 1 was obtained by dividing the analyzed data into training sets and validation sets at a ratio of 7 : 3. The training sets were used to test the model, while the validation sets were used to validate the performance of the model without further cross validation.

4. Conclusions

In this work, through the analysis of human tissue samples and mouse tissue samples by iEESI-MS and human serum samples by DI-ESI-MS, we found significant changes in the

alteration of phospholipid composition upon liver cancer between humans and mice. Out of the detected phospholipids, six types of phospholipids (including PC(34:2), PC(36:4), PC (38:6), PC(36:2), PC(38:4) and PC(42:9)) were found to undergo similar alterations upon liver cancer in both human liver tissues and mouse liver tissues as well as in human serum. Our results indicate that these six phospholipids can be used as a minimal panel of differential metabolites or for the rapid molecular diagnosis of liver cancer with high accuracy, sensitivity and specificity by direct iEESI-MS analysis.

Conflicts of interest

There are no conflicts to declare.

Acknowledgements

References

1 X. Ma, Y. T. Tan, Y. Yang, J. Gao, H. L. Li, W. Zheng, Q. Lan, N. Rothman, X. O. Shu and Y. B. Xiang, *Int. J. Cancer*, 2018, **143**, 1896–1903.

2 J. Chen, W. Wang, S. Lv, P. Yin, X. Zhao, X. Lu, F. Zhang and G. Xu, *Anal. Chim. Acta*, 2009, **650**, 3–9.

3 L. Bakiri and E. F. Wagner, *Mol. Oncol.*, 2013, **7**, 206–223.

4 F. Connor, T. F. Rayner, S. J. Aitken, C. Feig, M. Lukk, J. Santoyo-Lopez and D. T. Odom, *J. Hepatol.*, 2018, **69**, 840–850.

5 C. Coulouarn, V. M. Factor, E. A. Conner and S. S. Thorgeirsson, *Carcinogenesis*, 2011, **32**, 1434–1440.

6 U. H. Weidle, D. Schmid, F. Birzele and U. Brinkmann, *Cancer Genomics Proteomics*, 2020, **17**, 1–21.

7 K. Schulze, S. Imbeaud, E. Letouze, L. B. Alexandrov, J. Calderaro, S. Rebouissou, G. Couchy, C. Meiller, J. Shinde, F. Soysouvanh, A. L. Calatayud, R. Pinyol, L. Pelletier, C. Balabaud, A. Laurent, J. F. Blanc, V. Mazzaferro, F. Calvo, A. Villanueva, J. C. Nault, P. Bioulac-Sage, M. R. Stratton, J. M. Llovet and J. Zucman-Rossi, *Nat. Genet.*, 2015, **47**, 505–511.

8 L. Zender, W. Xue, J. Zuber, C. P. Semighini, A. Krasnitz, B. Ma, P. Zender, S. Kubicka, J. M. Luk, P. Schirmacher, W. R. McCombie, M. Wigler, J. Hicks, G. J. Hannon, S. Powers and S. W. Lowe, *Cell*, 2008, **135**, 852–864.

9 J. M. Mato, F. Elortza, S. C. Lu, V. Brun, A. Paradela and F. J. Corrales, *Expert Rev. Proteomics*, 2018, **15**, 749–756.

10 L. Shan, Y. A. Chen, L. Davis, G. Han, W. Zhu, A. D. Molina, H. Arango, J. P. LaPolla, M. S. Hoffman, T. Sellers, T. Kirby, S. V. Nicosia and R. Sutphen, *PLoS One*, 2012, **7**, e46846.

11 I. DobrzyånSka, B. Szachowicz-Petelska, S. Sulkowski and Z. Figaszewski, *Mol. Cell. Biochem.*, 2005, **276**, 113–119.

12 R. Bandu, H. J. Mok and K. P. Kim, *Mass Spectrom. Rev.*, 2018, **37**, 107–138.

13 H. Zhang, K. Chingin, J. Li, H. Lu, K. Huang and H. Chen, *Anal. Chem.*, 2018, **90**, 12101–12107.

14 J. M. Wiseman, S. M. Puolitaival, Z. Takats, R. G. Cooks and R. M. Caprioli, *Angew. Chem., Int. Ed.*, 2005, **44**, 7094–7097.

15 S. N. Jackson, H. Y. Wang, A. S. Woods, M. Ugarov, T. Egan and J. A. Schultz, *J. Am. Soc. Mass Spectrom.*, 2005, **16**, 133–138.

16 K. Glunde, C. Jie and Z. M. Bhujwalla, *Cancer Res.*, 2004, **64**, 4270–4276.

17 E. Marien, M. Meister, T. Muley, S. Fieuws, S. Bordel, R. Derua, J. Spraggins, R. Van de Plas, J. Dehairs, J. Wouters, M. Bagadi, H. Dienemann, M. Thomas, P. A. Schnabel, R. M. Caprioli, E. Waelkens and J. V. Swinnen, *Int. J. Cancer*, 2015, **137**, 1539–1548.

18 A. K. Jarmuscha, V. Pirroa, Z. Bairda, E. M. Hattabb, A. A. Cohen-Gadolc and R. G. Cooks, *Proc. Natl. Acad. Sci. U. S. A.*, 2016, **113**, 1486–1491.

19 H. Zhang, K. Chingin, L. Zhu and H. Chen, *Anal. Chem.*, 2015, **87**, 2878–2883.

20 H. Zhang, H. Gu, F. Yan, N. Wang, Y. Wei, J. Xu and H. Chen, *Sci. Rep.*, 2013, **3**, 2495.

21 H. Zhang, L. Zhu, L. Luo, N. Wang, K. Chingin, X. Guo and H. Chen, *J. Agric. Food Chem.*, 2013, **61**, 10691–10698.

22 H. Lu, H. Zhang, K. Chingin, Y. Wei, J. Xu, M. Ke, K. Huang, S. Feng and H. Chen, *Anal. Chem.*, 2019, **91**, 10532–10540.

23 J. Xu, S. Xu, Y. Xiao, K. Chingin, H. Lu, R. Yan and H. Chen, *Anal. Chem.*, 2017, **89**, 11252–11258.

24 S. Guo, Y. Wang, D. Zhou and Z. Li, *Sci. Rep.*, 2014, **4**, 5959.

25 Y. Wei, L. Chen, W. Zhou, K. Chingin, Y. Ouyang, T. Zhu, H. Wen, J. Ding, J. Xu and H. Chen, *Sci. Rep.*, 2015, **5**, 10077.

26 Y. Ouyang, J. Liu, B. Nie, N. Dong, X. Chen, L. Chen and Y. Wei, *RSC Adv.*, 2017, **7**, 56044–56053.

27 Y. Morita, T. Sakaguchi, K. Ikegami, N. Goto-Inoue, T. Hayasaka, V. T. Hang, H. Tanaka, T. Harada, Y. Shibasaki and A. Suzuki, *J. Hepatol.*, 2013, **59**, 292–299.

28 T. Yi, L. Zhu, W. Peng, X. He, H. Chen, J. Li, T. Yu, Z. Liang, Z. Zhao and H. Chen, *LWT – Food Sci. Technol.*, 2015, **62**, 194–201.

29 A. Patras, N. P. Brunton, G. Downey, A. Rawson, K. Warriner and G. Gernigon, *J. Food Compos. Anal.*, 2011, **24**, 250–256.

30 E. Szymanska, E. Saccenti, A. K. Smilde and J. A. Westerhuis, *Metabolomics*, 2012, **8**, 3–16.

31 S. Krautbauer, E. M. Meier, L. Rein-Fischboeck, R. Pohl, T. S. Weiss, A. Sigruener, C. Aslanidis, G. Liebisch and C. Buechler, *Biochim. Biophys. Acta*, 2016, **1861**, 1767–1774.

32 W. K. Chan, H. M. Lee, T. H. Lee, C. Kang and S. G. Yong, *Cancer Res.*, 2002, **62**, 6312–6317.

33 L. A. Balaceanu, *World J. Clin. Cases*, 2019, **7**, 1367–1382.

34 L. Zhou, J. Liu and F. Luo, *World J. Gastroenterol.*, 2006, **12**, 1175–1181.

35 R. C. Deo, M. Şahin, J. F. Adamowski and J. Mi, *Renewable Sustainable Energy Rev.*, 2019, **104**, 235–261.

36 P. Luo, P. Yin, R. Hua, Y. Tan, Z. Li, G. Qiu, Z. Yin, X. Xie, X. Wang, W. Chen, L. Zhou, X. Wang, Y. Li, H. Chen, L. Gao, X. Lu, T. Wu, H. Wang, J. Niu and G. Xu, *Hepatology*, 2018, **67**, 662–675.